An Optimal Motion Planning Method for Computer-Assisted Surgical Training

ARTICLE *in* APPLIED SOFT COMPUTING · NOVEMBER 2014

Impact Factor: 2.81 · DOI: 10.1016/j.asoc.2014.08.054

Liana Napalkova

Autonomous University of Barcelona

Jerzy W Rozenblit

The University of Arizona

George Hwang

The University of Arizona

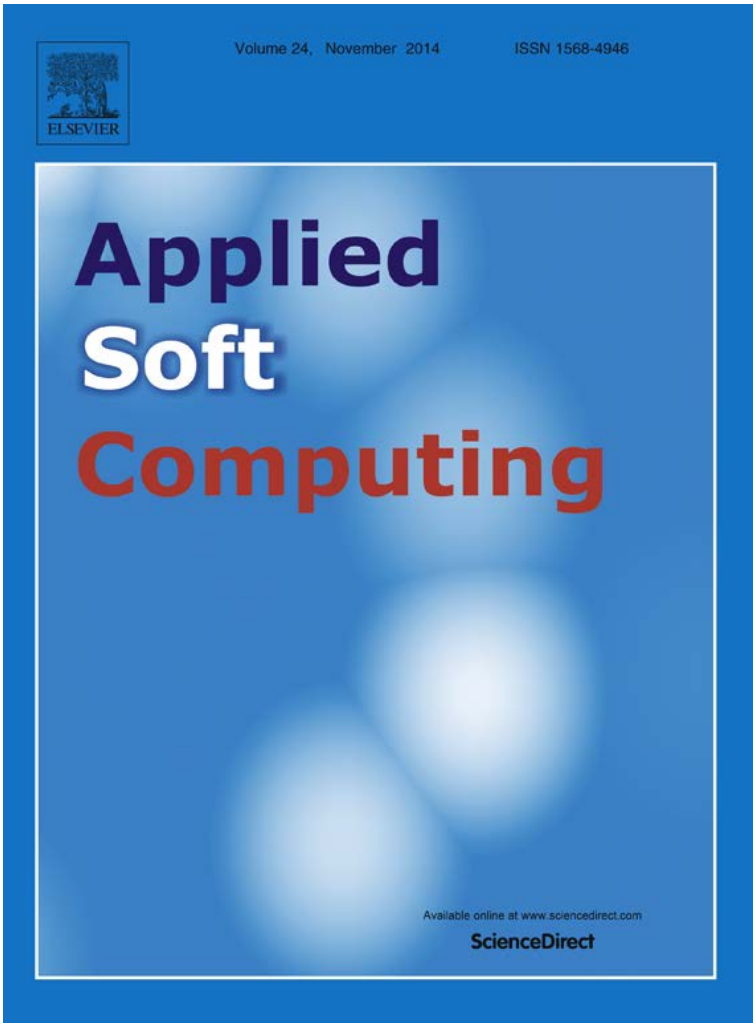

Applied Soft Computing 24 (2014) 889–899

Contents lists available at ScienceDirect

Applied Soft Computing

journal homepage: www.elsevier.com/locate/asoc

An optimal motion planning method for computer-assisted surgical training

Liana Napalkova[a,*], Jerzy W. Rozenblit[b,c], George Hwang[b], Allan J. Hamilton[b,c], Liana Suantak[b]

[a] Department of Telecommunications and Systems Engineering, The Autonomous University of Barcelona, Carrer Emprius 2, Sabadell, Barcelona 08202, Spain
[b] Department of Electrical and Computer Engineering, The University of Arizona, 1230 E. Speedway Boulevard, Tucson, AZ 85721, USA
[c] Department of Surgery, College of Medicine, The University of Arizona, 1501 N. Campbell Avenue, Tucson, AZ 85724, USA

ARTICLE INFO

Article history:
Received 7 December 2012
Received in revised form 21 August 2014
Accepted 22 August 2014
Available online 30 August 2014

Keywords:
Computer-assisted surgical training
Laparoscopic surgery
Optimal motion planning
Performance assessment

ABSTRACT

This paper focuses on the development and validation of an optimal motion planning method for computer-assisted surgical training. The context of this work is the development of new-generation systems that combine artificial intelligence and computer vision techniques in order to adjust the learning process to specific needs of a trainee, while preventing a trainee from the memorization of particular task settings. The problem described in the paper is the generation of shortest, collision-free trajectories for laparoscopic instrument movements in the rigid block world used for hand–eye coordination tasks. Optimal trajectories are displayed on a monitor to provide continuous visual guidance for optimal navigation of instruments. The key result of the work is a framework for the transition from surgical training systems in which users are dependent on predefined task settings and lack guidance for optimal navigation of laparoscopic instruments, to the so called intelligent systems that can potentially deliver the utmost flexibility to the learning process. A preliminary empirical evaluation of the developed optimal motion planning method has demonstrated the increase of total scores measured by total time taken to complete the task, and the instrument movement economy ratio. Experimentation with different task settings and the technical enhancement of the visual guidance are subjects of future research.

1. Introduction

Over the past two decades, a variety of surgical training systems for minimally invasive surgery (MIS) have been proposed and developed [1–8]. This effort has been motivated by the fact that the traditional way of learning surgery has come under intense scrutiny; the operating room is a setting where surgical procedures take place rather than a learning environment where mistakes could occur and would be corrected [9]. Limited time and a highly stressful surgical environment complicate the training process.

Typical challenges of MIS procedures include a restricted field of vision, hand–eye coordination problems, limited flexibility of laparoscopic instruments, and the lack of tactile sensation [10]. Thus, the primary goal of surgical training systems is to bring a trainee to a higher level of proficiency without putting patients at risk in the operating room. This can potentially reduce risks, improve surgical outcomes, and mitigate trainees' stress associated with insufficient experience in practicing laparoscopic skills.

Simulation training develops proficiency in surgical procedures such as suturing, laparoscopy and angiography [11–13]. Seymour et al. report that residents trained with virtual reality (VR) methods are able to perform a laparoscopic cholecystectomy 29% faster than residents who train with just the standard box trainers [13], while trainees without VR training were five times more likely to injure the gallbladder or inadvertently burn and coagulate adjacent tissue. A large multivariate analysis has demonstrated that a surgeon's experience is the single most important factor associated with positive outcomes in laparoscopic cholecystectomy procedures [14,15]. The learning curve also proves critical: 90% of injuries occurred within the first 30 cholecystectomies performed by a surgeon [15]. Since it plays such an important role in adverse outcomes, the speed with which technical proficiency is acquired becomes an important design consideration in the creation of

* Corresponding author. Tel.: +34 686397998.
E-mail addresses: liana.napalkova@uab.cat, liana.napalkova@gmail.com (L. Napalkova), jr@ece.arizona.edu (J.W. Rozenblit), hwangg@email.arizona.edu (G. Hwang), allan@surgery.arizona.edu (A.J. Hamilton), lianason@email.arizona.edu (L. Suantak).

http://dx.doi.org/10.1016/j.asoc.2014.08.054
1568-4946/

platforms to teach surgical skills. Studies have demonstrated that VR simulators employing haptic feedback quantitatively differentiate psychomotor skill acquisition between experts and novice surgeons [16,17]. Determining proficiency is an important factor in timing the transition of surgical trainees from simulation training to actual procedures in the operating room.

Sensory feedback plays a crucial role in the motor control of instruments and tissue manipulation during laparoscopic surgery [18]. Indeed, the lack of haptic feedback in most surgical robotic systems is often reported by expert surgeons to be detrimental to their surgical technique [19]. Nonetheless, the introduction of haptics in surgical simulation training seems to improve surgical skill acquisition [20,21]. Force feedback in a VR laparoscopic suturing task has been shown to shorten completion time, reduce the amount of force inadvertently applied to tissues, and improve the accuracy of suture placement [22]. More recently, haptics has also be shown to quantitatively enhance robotically assisted knot-tying with fine sutures [23].

We report on a methodology that combines an optimal motion planning system with the standardized objective assessment capabilities offered by VR trainers while still permitting trainees to use real surgical instrumentation that offers the same sensory feedback as traditional box trainers or actual surgery. VR trainers suffer from: (1) a lack of high-fidelity in the applied instrumentation (e.g., a forceps has same underlying haptic mechanisms as a scissors), (2) highly representational computer-derived depiction of anatomy, and (3) a poor approximation of the tensile and deformability characteristics of different tissues. While valuable quantitative information is obtained from haptically driven VR trainers, it is still data that are ultimately derived from a highly simplified and abstracted surgical "reality".

Our computer assisted surgical trainer (CAST) incorporates haptic feedback for the purposes of shaping and guiding surgical movement but it also allows trainees to learn technique use, the actual surgical instrumentation and laparoscopic viewing equipment they will employ in the performance of actual procedures [10]. Harnessing this to sophisticated artificial tissue modules that offer tensile, anatomic, and vascular properties more closely approximating those of actual animal or human tissue permits CAST to offer an environment with higher fidelity and more realism in which to quantitatively collect and analyze a trainee's acquisition of laparoscopic skills and make determinations about proficiency in those techniques.

The remainder of the paper is organized as follows: Section 2 introduces the taxonomy of surgical training systems in order to categorize existing trainers and define a group of systems that fall into the scope of our research. Section 3 provides the mathematical formulation of the optimal motion planning problem that we consider as part of surgical training procedure. Conceptual design and motivation of the problem solving method is given in Section 4. In Section 5, we implement the proposed motion planning method that generates optimal, collision-free trajectories for different task settings. Section 6 validates the developed method based on three test cases. The case study of the CAST system is provided in Section 7. Finally, Section 8 concludes the paper with a summary and discussion of further research.

2. Taxonomy of surgical training systems

The key feature that characterizes any existing surgical training system is the way in which the concept of a supervisor is represented. Based on this classification, we distinguish four different types of systems:

(a) Self-supervised training systems in which a trainee performs a self-assessment in a subjective fashion, based on analyzing the results achieved through the self-learning process.
(b) Expert knowledge-based training systems that allow performance assessment with respect to the expert-derived proficiency levels specified for laparoscopy tasks.
(c) Competitive training systems in which trainees compete with one another in a game-like setting and compare the results with those of their competitors.
(d) Intelligent training systems in which the trainee receives continuous guidance on optimal navigation of laparoscopic instruments and his or her performance is evaluated with respect to optimal solutions that are found by artificial intelligence (AI) techniques.

Nowadays, laparoscopy teaching is mainly done with the assistance of surgical training systems related to the first three categories. Typical examples of self-supervised training systems are basket trainers [2,3,24] which usually consist of a box with holes for laparoscopic instruments and a camera displaying an image from an enclosed space meant to simulate the abdominal cavity. Due to the lack of guidance toward the improvement of laparoscopic skills, basket trainers can only be used under the supervision of experts or can serve as secondary trainers.

Commercial systems such as LapSim (Surgical Science) [6,25] and LAP Mentor (Simbionix) [7] are also classified as self-supervised training systems. Although several research studies attempted to set proficiency levels for the tasks, standardized proficiency information has not yet been uploaded in these systems [26,27]. Therefore, if expert surgeons are unavailable, LapSim and LAP Mentor can only provide a subjective assessment based on analyzing preliminary results of the trainees task performance.

Expert, knowledge-based training systems are rapidly emerging in the market [1,4,5,8,28]. Such systems demonstrate a significant advance over the self-supervised training systems since the trainee is allowed to enhance his or her laparoscopic skills by reaching predefined (and usually standardized) proficiency levels for the learning tasks [17].

The most widely known expert knowledge-based training systems are as follows: McGill Inanimate System for Training and Evaluation of Laparoscopic Skills (MISTELS) [4], Computer-Enhanced Laparoscopic Training System (CELTS) [1], FLS Laparoscopic Trainer Box [28] and Minimally Invasive Surgical Trainer-Virtual Reality (MIST-VR, Mentice) [5]. In particular, MISTELS objectively grades performance of the laparoscopic tasks based on the cutoff time and penalty score in order to help the trainee target areas requiring additional attention [8]. CELTS is equipped with an expert performance baseline database to provide standardized performance scoring. In the FLS Laparoscopic Trainer Box, the trainee is allowed to begin learning the next task after the proficiency that is measured in time, number of repetitions and number of errors, is demonstrated for the current task. Finally, MIST-VR is also classified as an expert knowledge-based training system since the benchmark proficiency levels have been recently established for it by experienced physicians who are members of the Society of American Gastrointestinal Endoscopic Surgeons (SAGES) [29].

Although game-based learning has been widely applied to different fields, the competitive surgical training systems are just emerging in the research literature. One of such systems is Head2Head (Verefi Technologies) [30]. In this system, trainees are assessed on their ability to perform basic laparoscopic tasks in the virtual environment. The trainee with the most wins in a set of several rounds receives a higher score. Performance of trainees is measured with respect to the speed, accuracy, and tool movement efficiency. Although such systems benefit from engaging, focusing and motivating trainees, they are deficient in recognizing that each

trainee requires a different number of rounds to acquire laparoscopic psychomotor skills. Therefore, competitive surgical training systems have more potential as secondary trainers and cannot be used as a unique training tool.

The development of intelligent surgical training systems is a novel research direction that is expected to play an increasingly important role in teaching laparoscopy skills. The aim of such systems is to provide continuous guidance for optimal, safe navigation along with augmented visual and haptic sensory information. Also, it is important to assess performance based on the information on optimal solutions for learning exercises. To our knowledge, currently there exists only one commercial system called RapidFire/SmartTutor (Verefi Technologies, Inc.) [31], which can optimize learning conditions for a trainee and adapt to the trainees skill level based on adjusting the difficulty of the task in real time [30]. RapidFire/SmartTutor still lacks some features of an intelligent training system such as (1) the independence of the expert surgeons' definition of proficiency and (2) the ability to provide continuous guidance on optimal, collision-free navigation of laparoscopic instruments.

The literature shows that skill proficiency information is used in both expert knowledge-based and intelligent training systems in order to give an overall picture of where the trainee is in the learning process, and to define the moment when the trainee is allowed to perform surgeries on real patients. However, the limitation of expert knowledge-based training systems is that proficiency can only be established for fixed task settings. If the settings have changed, expert surgeons should update the proficiency information, which could take additional time and cost.

Our research is focused on the development of a novel intelligent training system that benefits from high flexibility and independence of expert surgeons' active assistance. In this paper, we present and validate the method for optimal instrument movement guidance. The scientific novelty of this research consists in integrating this method into CAST in order to efficiently guide trainees toward the learning process. CAST is empowered with the capability to derive proficiency levels from optimal solutions found by our motion planning method. This can be performed by the system each time the task settings are changed. We expect that the integration of CAST into the medical learning process can significantly reduce total time and cost used for learning laparoscopy skills. The long term benefit will be improved surgical skills and operative outcomes.

3. Problem statement

In this section, we introduce the notation and formulate the motion planning problem.

Let $s_i(t)$ define a configuration that describes the state of the instrument i in the three dimensional 3D workspace $\mathcal{W}$ at time t, where $1, I$ and I is the number of instruments.

The configuration space $\mathcal{C}$ that represents the set of all possible states of the instruments is a union of configuration spaces $\bigcup_{i=1}^{I}\mathcal{C}_i$. Let also define the concave obstacle space $\mathcal{B}$ (known as the "no-fly" zone) that is composed of convex rigid obstacles $\bigcup_{j=1}^{J}\mathcal{B}_j$, where J is a number of obstacles. The set of configurations that avoid collision with obstacles is called the free space $\mathcal{C}_{free}$ defined as $\mathcal{C}_{free} = \mathcal{C} - \mathcal{B}$. Both $\mathcal{C}$ and $\mathcal{B}$ are represented as a mesh of tetrahedrons (see Section 5.1).

Since laparoscopic instruments are fixed at the pivot points, their movements are limited to three degrees of freedom (DOF) with a reduced range of motion. Thus, each configuration $s_i(t)$ of the ith instrument at time t can be represented using three parameters: pitch $\alpha_i(t)$, yaw $\beta_i(t)$, and insertion depth $\gamma_i(t)$. The pitch and yaw describe a limited inclination of the shaft pivoted through the incision, while the insertion depth determines translation along the shaft of the instrument. The rotation is not considered, because it does not change the position of the instrument in the workspace.

Given these definitions, the motion planning problem is formulated as follows: For each ith laparoscopic instrument, find a sequential set of configurations $S_i \in \mathcal{C}_{free}$ assigned to time values $t \in [0, T]$ such that:

(a) all targets are involved,
(b) the total length of the curve connecting all targets is the minimum of all possible path lengths,
(c) no $s_i(t)$ intersects any obstacle in $\mathcal{B}$, and
(d) $s_i(t)$ satisfies the non-penetration constraint (i.e., two laparoscopic instruments must not share the same space), where $s_i(0)$ and $s_i(T)$ are the start and goal configurations, respectively.

4. Conceptual design of the optimal motion planning method

The following steps were used to design the optimal motion planning method for solving the above-formulated problem: (1) representation of the obstacle space, (2) definition of the search strategy, and (3) selection of techniques that constitute the method.

To define the proper representation approach, the features of obstacle spaces used in laparoscopic training were analyzed. It was found that solid static obstacles and realistic soft tissues that are subject to predictable deformations are typically used for teaching laparoscopy skills [4,26,32]. Additionally, one must take into account the fact that moving instruments might collide in the operating space. Since this paper focuses on modeling solid static obstacles with dynamic instruments (i.e., multi-movers problem), our choice came down to the following space representation approaches: grid, cell tree, scalar function, mathematical programming, artificial neural networks, and polyhedrons [33].

The grid method decomposes the space into equally sized cells. The disadvantage of this method is that the approximation of curved shapes requires increasing the number of cells enormously while decreasing their size. This eliminates the applicability of exact algorithms while applicable heuristics cannot guarantee the optimality of solutions. The cell tree overcomes the disadvantage of the grid method by dividing the space into a smaller number of cells. However, the lack of homogeneity complicates the computation of adjacency between cells.

Scalar functions are used in combination with the potential-field method. This method, however, is likely to be trapped in a local optimum. Moreover, it becomes less efficient when concave shapes of obstacles and geometrical properties of laparoscopic instruments are considered. Mathematical programming uses inequality constraints to describe the shapes of obstacles. In the case of complex curved shapes, it can be difficult to formulate all the constraints and solve the related nonlinear optimization problem using a numerical method.

In artificial neural networks, the input data correspond to actual positions of instruments, while the output data provide next positions taking into account distances from obstacles. The accuracy of this representation strongly depends on the network design and the efficiency of the neural learning algorithm. This also restricts the problem solving to the methods that solely rely on outputs of the neural network to determine the search direction without using analytical expressions. Finally, polyhedral representation is based on approximating the space with a union of homogeneous polyhedrons.

In our particular domain of interest, the approximation with tetrahedrons benefits from high accuracy and simplicity, which perfectly conforms to the class of surgical training problems. After

the polyhedral representation was chosen, the next step was to select an appropriate search strategy (either online or offline [34]). Online search is based on analyzing a local space for making each movement of the instrument in an uncertain environment. This, however, could produce multiple backward and forward movements, which would negatively influence the surgical training procedure. Conversely, the offline search strategy can provide a global perspective for solving the problem. Although offline search algorithms are unable to deal with uncertain obstacle spaces, this disadvantage does not contradict our requirements because the locations of obstacles are known and small oscillations can be easily modeled by extending the boundaries of static obstacles. If laparoscopic instruments move toward prescribed optimal trajectories, all the collisions between them can be prevented a priori by assigning the average speed to these instruments. Thus, it can be argued that the offline search strategy better suits the conditions of laparoscopic training where the emphasis should be placed on teaching students to capture the problem features from the global perspective. It should be noted, however, that online search strategies can be more beneficial in cutting tasks, where irreversible deformations of the tissue occur.

Finally, techniques that need to constitute the optimal motion planning method and comply with the offline search paradigm were selected. Since a polyhedral representation of the obstacles is used, the method should be able to deal with a very large number of tetrahedrons in the case of a high complexity of the obstacle space. Therefore, it was necessary to find a better trade-off between the exploration of the search space and exploitation of the accumulated search experience (i.e., search intensification and diversification, respectively) [35]. In order to tackle this issue, the decomposition approach that allows dividing the problem into easily manageable sub-problems was applied. According to this approach, the Delaunay tetrahedralization algorithm [36] is used to split obstacles into tetrahedrons and to derive the free space so that all tetrahedrons located in this free space comprise the search space of the optimal motion planning method. Dijkstra's algorithm [37] defines tetrahedrons that correspond to promising areas in the space. An enumerative combinatorics technique exhaustively explores the selected areas of interest to provide more accurate solution to the problem. Cubic spline methodology [38] helps in constructing realistic smooth paths to prevent zig-zag movements of the instruments. The explorational power of population-based heuristics, such as elitist genetic algorithm [39,40], is used to quickly find the near-optimal average speed for instrument movements in order to prevent collisions between them.

5. Implementation of the method

The optimal motion planning method for minimally invasive surgery (optMIS) was developed in accordance to the conceptual design described in the previous section. The method consists of the following sequential stages:

1. Shortest path planning: for each laparoscopic instrument find a set of configurations $S_i \in \mathcal{C}_{free}$ corresponding to a shortest path.
2. Time-optimal trajectory planning: assign time period t to each configuration $s_i(t) \in S_i$ in order to avoid collisions between the instruments.

5.1. Shortest path planning

The first step toward defining the shortest path S_i is to represent the workspace as a mesh of tetrahedrons. The goal is to decompose the workspace into simplicial complexes, i.e., a finite collection of indices and ordered tuples of vertices. For this, we apply the Delaunay tetrahedralization algorithm to each convex obstacle $\mathcal{B}_j$. The union DT_{obst} of simplicial complexes that decompose the concave hull of the obstacle points is obtained as follows:

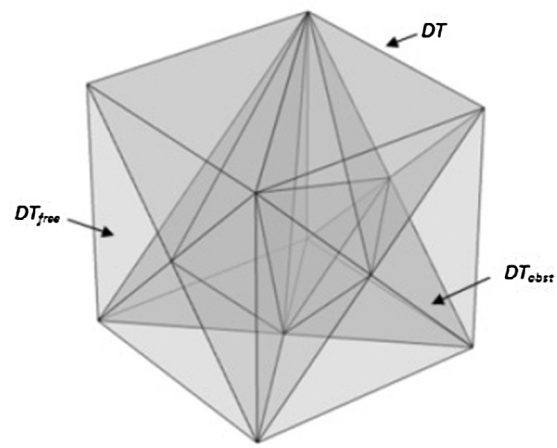

Fig. 1. Graphical representation of DT, DT_{free} and DT_{obst}.

$$DT_{obst} = \bigcup_{j=1}^{J} DT_j \tag{1}$$

where DT_j is a simplicial complex that represents the jth obstacle. Then, a simplicial complex DT_{free} that corresponds to the free space $\mathcal{C}_{free}$ is defined by decomposing the workspace $\mathcal{W}$ into a mesh of tetrahedrons DT and subtracting DT_{obst} from it:

$$DT_{free} = DT - DT_{obst} \tag{2}$$

A 3D graphic illustrating what are DT, DT_{free} and DT_{obst} is shown in Fig. 1. DT_{obst} is given in a dark-gray color, DT_{free} is represented as a space colored in light gray, while DT is a union of DT_{free} and DT_{obst}.

The vertices of tetrahedrons DT are generated randomly using a uniform distribution. In contrast to the methods of alpha shapes [41,42], which require defining global or local threshold alpha, our approach provides more flexibility in modeling complex obstacle spaces and is independent of additional parameters. Once the workspace has been decomposed, Dijkstra's algorithm is applied to find the shortest continuous channel of tetrahedrons $Q_i = \{q_i^1, \ldots, q_i^N\} \in DT_{free}$ between start and target configurations, where N is a number of tetrahedrons in a channel Q_i. Since Dijkstras algorithm works on graphs, vertices of a graph are represented as centroids of tetrahedrons that correspond to the free space $\mathcal{C}_{free}$. Thus, at each iteration the algorithm picks the unvisited vertex (centroid) with the lowest-distance, calculates the distance through it to each unvisited neighbor and updates the neighbor's distance if a smaller one is found. The length of the channel $L(Q_i)$ is calculated as the sum of distances between centroids of the tetrahedrons. A set of configurations $S_i = \{s_i^1, \ldots, s_i^N\} \in Q_i$ corresponding to the shortest path is built to satisfy the following constraints Ω for $i = \overline{1, I}$ and $n = \overline{1, N}$:

$$\Omega : \begin{cases} s_i^n \bigcap \mathcal{B} = \emptyset \\ \alpha_i^n \in [\alpha_i^{\min}, \alpha_i^{\max}] \\ \beta_i^n \in [\beta_i^{\min}, \beta_i^{\max}] \\ \gamma_i^n \in [\gamma_i^{\min}, \gamma_i^{\max}] \end{cases} \tag{3}$$

The first constraint eliminates collisions with obstacles when the ith instrument is at the configuration s_i^n, with the provision that the instrument be geometrically represented as a cylinder with the radius ρ_i. The second, third, and fourth constraints are used to check whether the pitch and yaw angles as well as the insertion depth stay within the range between the lower and upper bounds.

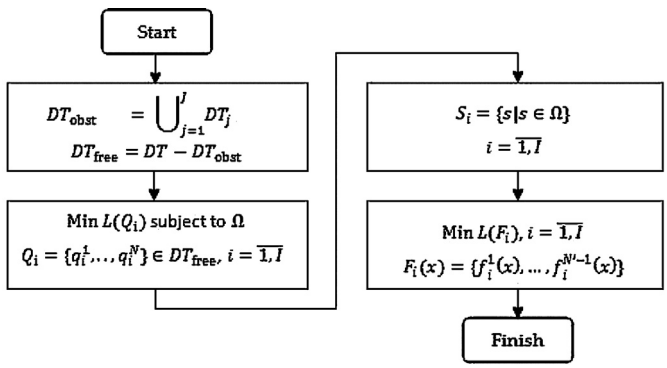

Fig. 2. Flowchart of the shortest path planning algorithm.

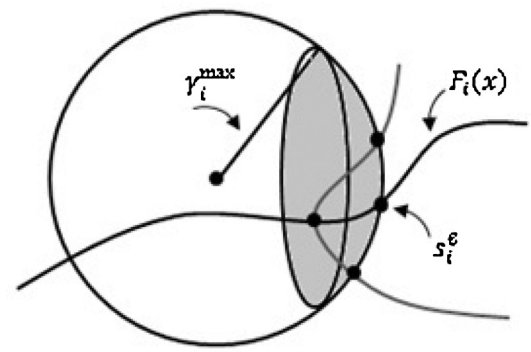

Fig. 3. Definition of the intersection configurations.

As a result, our Dijkstra's algorithm always provides the shortest feasible channel without the need to solve more time-consuming k-shortest paths problem [43].

The next step is to construct the shortest curve through the data points corresponding to $S_i = \{s_i^n | s_i^n \in \Omega\}$. An enumerative combinatorics technique is used to evaluate all combinations of the data points and find the one that gives the minimal length of the curve. The cubic spline methodology is applied to fit third-order polynomials between the data points providing that the curve obtained is continuous and smooth, i.e.:

$$F_i(x) = \{f_i^1(x), \ldots, f_i^{(N'-1)}(x)\}$$
$$f_i^n(x) = a_i^n(x - x_i^n)^3 + b_i^n(x - x_i^n)^2 + c_i^n(x - x_i^n) + d_i^n \quad x_n \le x \le x_{n+1} \tag{4}$$

where $F_i(x)$ is a piecewise function, $f_i^n(x)$ is a cubic polynomial; $x \in \Re^3$ is a position in 3D Cartesian space; a, b, c and d are coefficients; N' is the number of data points that satisfy the constraints Ω and $N' \le N$.

The obtained curves are then used to interpolate the positions of laparoscopic instruments within the range of targets. The flowchart of the above-described algorithm is given in Fig. 2.

5.2. Time-optimal trajectory planning

In this stage, a time law is specified on shortest paths $F_i(x)$ in order to avoid collisions between instruments. The stage consists of the following two steps:

1. Define the configurations at which laparoscopic instruments intersect;
2. Assign a time value to each intersection configuration in order to prevent collisions between the instruments.

In order to detect the intersection points of the instruments, the configuration spaces $\mathcal{C}_i$ are represented in terms of spheres with radii equal to γ_i^{max}. The collision area is composed of spherical caps that are found analytically by combining the equations of spheres. Bounding points are defined for the intervals of shortest paths that belong to the collision area. These points are then assigned to the intersection configurations:

$$S_i^{int} = \{s_i^1, \ldots, s_i^L\} \subset S_i \tag{5}$$

where L is a number of intersections (see Fig. 3).

Once the first step is completed, an elitist genetic algorithm (GA) is applied to find the periods of time t when the intersection configurations $s_i \in S_i^{int}$ should be reached. Formally, the algorithm can be described as follows.

Let $P^\tau = \{p^1, \ldots, p^Z\}$ be a population at generation τ that consists of Z chromosomes. Each chromosome in P^τ is represented by a binary string such as:

$$p^z = (p_{m-1}^z p_{m-2}^z \ldots p_1^z p_0^z) \in \{0, 1\}^m \tag{6}$$

where z is the index of a string; m is a length of a string calculated as L multiplied by the number of genes necessary to encode T; p_m^z is a gene at locus m. Binary strings p^l are used to encode time values $t \in [0, T]$ for $s_i^l(t) \in S_i^{int}$, $l = \overline{1,L}$ and $i = \overline{1,I}$. The fitness function Fit^z operates to minimize a weighted sum of the following components:

(a) Fit_1^z: the time delay between placing multiple laparoscopic instruments at each intersection point.
(b) Fit_2^z: the rate by which the magnitude of velocity is changed along the paths.
(c) Fit_3^z: the total time T during which all goal positions are accessed.

The penalty function is applied to infeasible chromosomes in order to decrease their survival probability. A chromosome p^z is considered to be infeasible if the time delay Fit_1^z is lower than a predefined lower bound Fit_1^{min}.

The performance of the elitist GA algorithm is controlled by the genetic operator $\mathcal{G}$ that implements iterative transitions between populations according to:

$$P^{(\tau+1)} \sim \mathcal{G}(P^\tau) \tag{7}$$

where $\sim$ is an equivalence relation. This operator is composed of four sub-operators, namely the stochastic universal sampling ($\mathcal{A}_s$), the uniform crossover ($\mathcal{A}_c$), the mutation ($\mathcal{A}_m$) and the reproduction ($\mathcal{A}_r$) so that:

$$\mathcal{G} = \mathcal{A}_s \circ \mathcal{A}_c \circ \mathcal{A}_m \circ \mathcal{A}_r. \tag{8}$$

External archiving is introduced as the elitist mechanism to avoid the loss of the best solution during the evolution process. The external archive is updated by a new best solution Fit^z if its fitness value is lower than the value of current best solution Fit^{min}.

The elitist GA is automatically terminated once the number d^* of generations with a constant best solution is equal to the predefined value d^* within some threshold. The flowchart of GA is shown in Fig. 4.

The GA outputs time values that we further use to estimate the instruments' average speed at particular segments of the shortest paths.

6. Validation of the method

Three test cases were designed to evaluate the search efficiency of the optMIS method. Test case 1 was used to analyze how search

Table 1
Cartesian coordinates of target points (in cm).

Targets		OS1	OS2	OS3	OS4	OS5
Left	Start	1, 1, 1.5	2, 11, 1.5	8, 24, 0	8, 24, 1.5	1, 1, 0
Left	Goal	10.5, 20.5, 1.5	11, 15.5, 1.5	9, 1, 1.5	10, 10, 0	8, 16, 9.5
Right	Start	1, 1, 1.5	11, 1, 1.5	23, 21, 1.5	23, 21, 0	8, 13, 0
Right	Goal	21, 6, 2.5	23, 21, 1.5	21, 6, 2.5	12, 1, 1.5	21.5, 10, 10.5

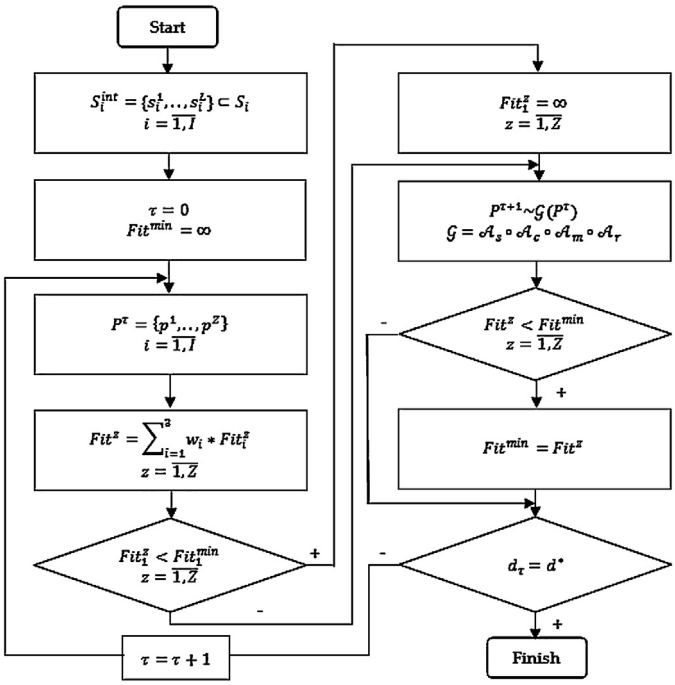

Fig. 4. Flowchart of the time-optimal trajectory planning algorithm.

space discretization influences the solution quality and run-time of the method. Test case 2 was aimed at investigating the impact of physical constraints on optimization results. Finally, the capability of the method to resolve collisions between moving instruments was verified in test case 3. All test cases were conducted on Intel Core i3 2.40 GHz processor with 4 GB of RAM. The method was developed in MATLAB R2010b.

Five different obstacle spaces (OS1, . . ., OS5) were developed using cuboids, prisms, spheres, octahedrons, and concave polyhedral compounds. In each obstacle space, target points were specified for left and right laparoscopic instruments (see Table 1).

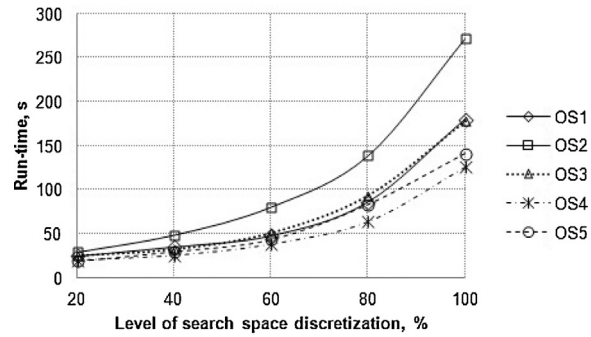

Fig. 6. Functional relationship between the run-time and search space discretization levels.

6.1. Test case 1

Five levels of search space discretization were defined, where the level of 100% corresponded to the most crowded space (i.e., higher number of particles). The performance of the method was evaluated by measuring the run-time of the method and shortest path lengths. In order to increase the number of candidate solutions and to verify the capability of the method to determine optimal search direction, physical constraints imposed on the laparoscopic instruments were relaxed in this test case.

As shown in Fig. 5 the values of shortest path lengths changed according to a function with a low steepness. The run-time, however, grew exponentially from 20 to 270 s (on average), while increasing the level of space discretization from 20% to 100% (Fig. 6). The proper trade-off between the run-time and solution quality was achieved at the level of 80%, which was, therefore, selected as a constant discretization level for further experiment. Fig. 7 illustrates the shortest paths obtained at the selected level of search space discretization. Because the bounds of obstacles can be controlled, the paths were allowed to be narrow.

6.2. Test case 2

In test case 2, laparoscopic instrument movements along the paths were modeled to identify those path segments that either

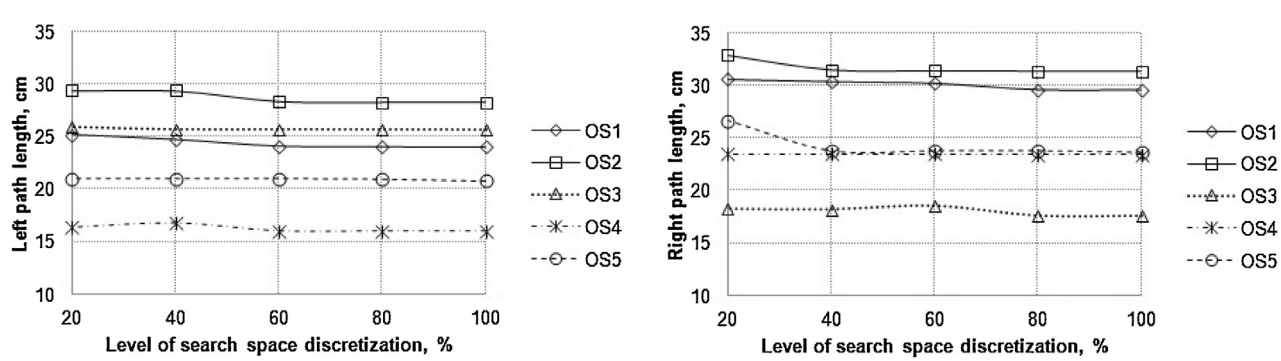

Fig. 5. Functional relationship between shortest path lengths and search space discretization levels.

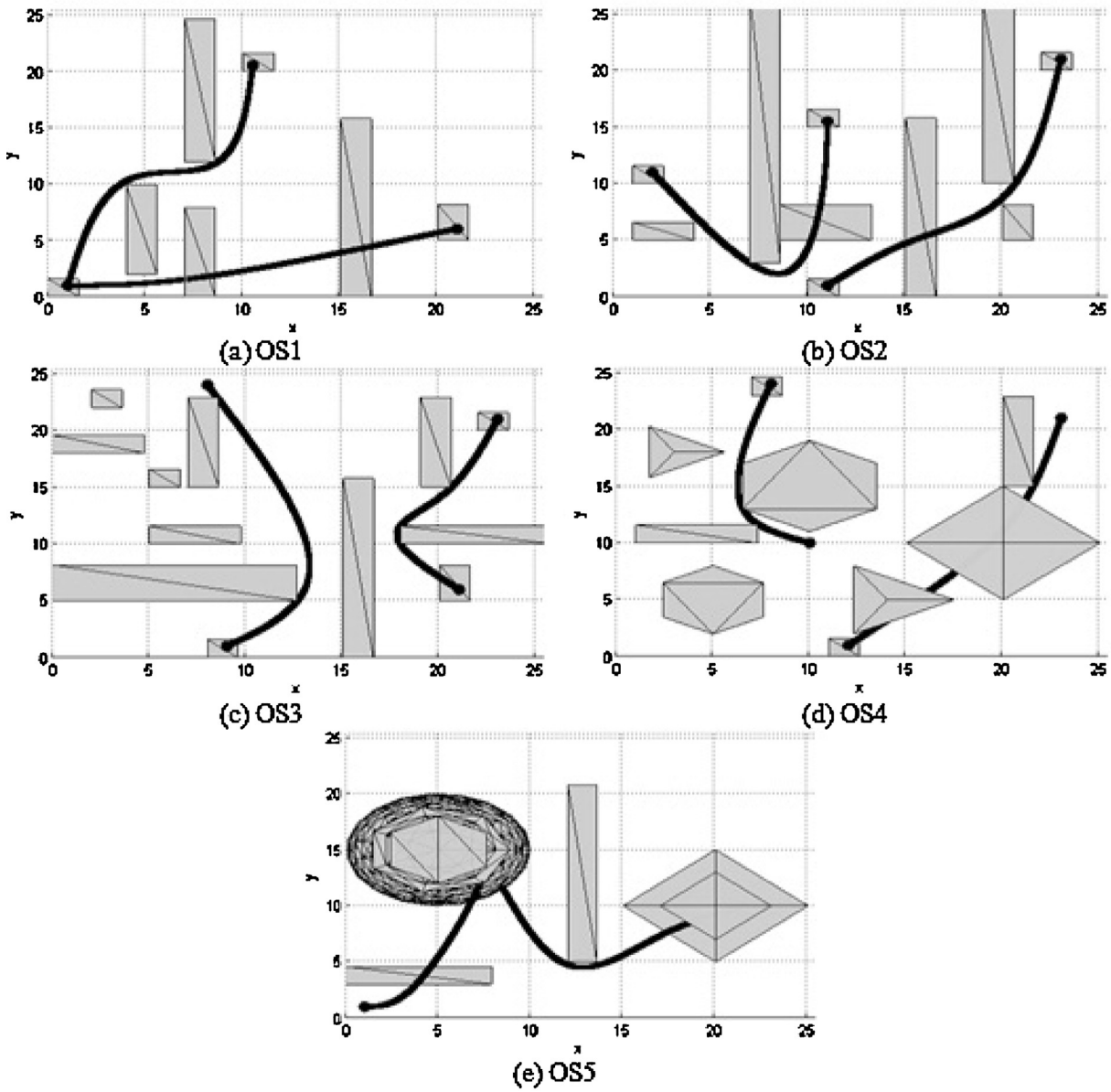

Fig. 7. 3D projection of shortest paths.

are unreachable by the instrument or result in collisions between the instrument and static obstacles.

Yaw angles for right and left instruments were restricted to 84.08° and 85.76°, while maximum insertion depths were equal to 23.06 cm and 24.56 cm, respectively. The radius of instruments was equal to 0.2 cm, while "*xyz*" coordinates of left and right fixtures were [3.71, −7.21, 15.36] cm and [20.34, −6.97, 15.76] cm, accordingly. To illustrate the impact of physical constraints on outputs of the optMIS method, we used obstacle spaces described in test case 1, while replacing unreachable target points with reachable ones (see Table 2).

It was found that the run-time of DA (Dijkstra's algorithm) and EC (enumerative combinatorics) functions for the constrained problem increased (on average) by 8 and 4 times, respectively (Table 3). This increase was due to the fact that we verified the feasibility of candidate solutions at each iteration of the method. Moreover, the run-time correlated with the number and shape of obstacles as well as with the reachability of target points. Therefore,

Table 2
Cartesian coordinates of reachable target points (in cm).

Targets		OS1	OS2	OS3	OS4	OS5
Left	Start	1, 1, 1.5	3, 6, 10.2	5.2, 19, 16	10, 16, 15.5	1, 1, 0
Left	Goal	8, 7, 10.2	16, 3, 10.2	9, 1, 1.5	10, 10, 0	7.5, 12, 9.5
Right	Start	1, 1, 1.5	11, 1, 1.5	5, 6, 10.2	14, 15, 10	8, 15, 18
Right	Goal	21, 6, 2.5	21, 7, 2.5	21, 6, 2.5	12, 1, 1.5	21.5, 10, 10.5

Table 3
Run-time of the method's functions (in s).

Funct.	OS1	OS2	OS3	OS4	OS5
Constr.					
DA	38	58	82	50	69
EC	181	248	397	368	284
Unconstr.					
DA	6	6	9	9	6
EC	69	57	95	115	71

Table 4
Shortest path lengths (in cm).

Paths	OS1	OS2	OS3	OS4	OS5
Constr.					
Left	15.20	14.46	25.72	19.93	16.94
Right	30.39	21.41	20.81	17.40	17.71
Unconstr.					
Left	15.20	14.28	25.62	19.93	16.94
Right	29.62	21.41	20.31	16.70	16.50

the highest run-time value was obtained for OS3, where density of obstacles was higher than in other spaces.

It was also determined that for the constrained case, the length of the shortest left and right paths increased on average by 0.33% and 3.16%, respectively (Table 4).

Fig. 8 illustrates the difference in solutions found for constrained and unconstrained cases in OS5. To solve the constrained problem, the optMIS method generated paths using only those points that were reachable by laparoscopic instruments. Therefore, as shown in Fig. 8, the actual shortest path of the right instrument was defined as an infeasible solution in the constrained case. Instead, the method found the first available shortest path that fit the physical constraints (3).

6.3. Test case 3

In this test case, the elitist GA was applied to resolve collisions between two moving instruments. To model collisions, new target points were defined for OS1, i.e.:

1. Left targets: Start [8, 4, 10.5] cm, Goal [16, 14, 10.5] cm.
2. Right targets: Start [21, 6, 2.5] cm, Goal [8, 15, 10.5] cm.

Then, shortest paths were found to connect these target points (Fig. 9).

Next, the intersection points of the instruments were detected and the elitist GA was executed to assign time values to these

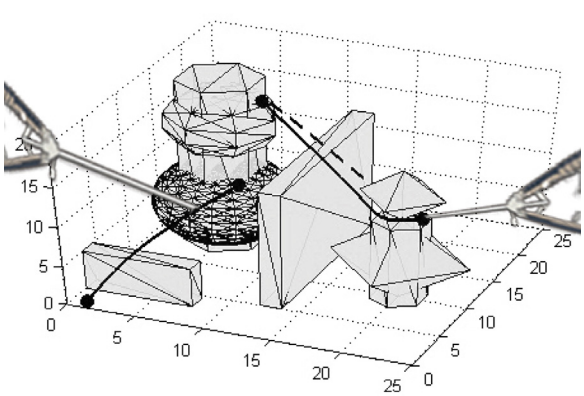

Fig. 8. Shortest feasible paths found for constrained (solid line) and unconstrained (dashed line) cases.

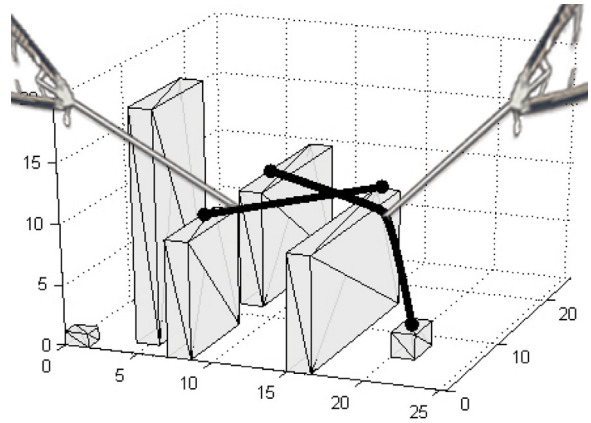

Fig. 9. Shortest feasible paths in OS1.

Table 5
Parameters of GA.

Parameter	Value
Crossover probability	0.7
Mutation probability	0.01
Nr of positions to encode the phenotype	5
Threshold	0.001
Nr of generations with constant best solution	10

Table 6
Time values (in arbitrary units).

Paths	Population size			
	20	50	70	100
Left	15, 24, 30	20, 29, 30	21, 30, 31	21, 30, 31
Right	10, 16, 17	9, 16, 17	13, 20, 21	13, 20, 21

points. Parameters of the GA are shown in Table 5. Sigma scaling was applied to avoid premature convergence of the GA. The algorithm was terminated after the best solution did not change over ten generations. The threshold of 0.001 was used to compute the degree of similarity between best solutions.

Table 6 summarizes time values found by the GA for different population sizes. Although the GA is a stochastic algorithm, only a single run was required to find feasible solution. As a result, in all cases the right instrument was moving faster than the left one to prevent collisions. Since all solutions were equally applicable in practice, this motivated us to further place the emphasis of the GA on the feasibility of a solution rather than on its optimality.

Fig. 10 shows performance graphs of GA for population sizes 50 and 100. Feasible solutions were found after 20 and 57 generations, respectively.

7. Case study

7.1. Study design

A case study was set up to validate practical applicability of our method and to demonstrate how visual guidance based on optimal navigation works and influences the operator. The authors completed hand–eye coordination tasks on the CAST system according to the following two scenarios:

(a) Scenario 1: The monitor displayed an image generated from the camera.
(b) Scenario 2: The visual guidance on optimal collision-free navigation was additionally displayed on the monitor.

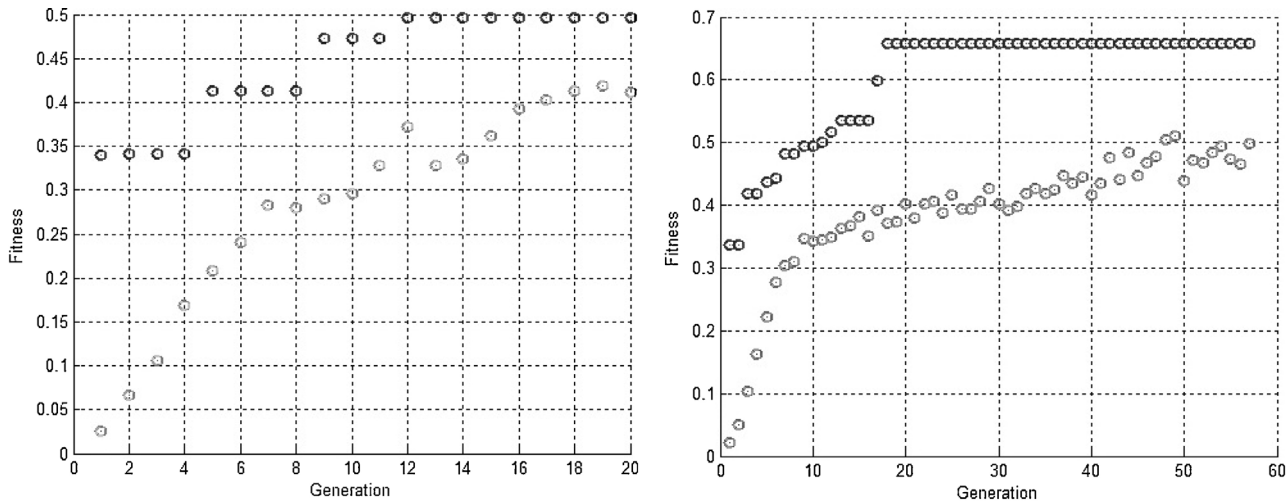

Fig. 10. Performance graphs of GA. Maximal fitness values (black circles), average fitness values (gray circles).

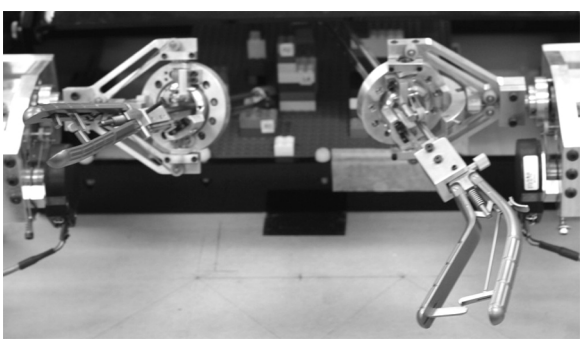

Fig. 11. Laparoscopic instruments mounted to fixtures.

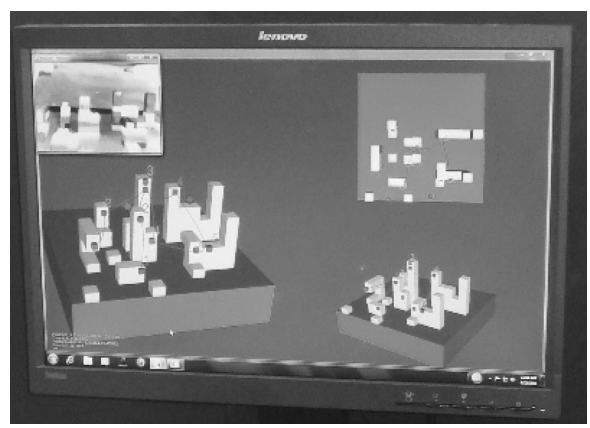

Fig. 12. LCD monitor displaying the image generated from the camera, virtual reality model and shortest paths.

It must be noted that the current implementation of the CAST hardware does not allow the "time" guidance. Therefore, in the proposed case study, the authors selected a hand–eye coordination task without collisions between the instruments. We plan to implement the "time" guidance as follows: a solution of GA should be converted into countdown clocks that pop up at intersection points for each instrument. For instance, if the left and right instruments should reach a collision point at periods 15 and 10, respectively, then two countdown clocks should be displayed on the monitor. Delays in reaching collision points should be saved to score performance of a user.

7.2. System setup

The CAST system consists of a laparoscopic trainer box, two fixtures to mount two Karl Storz laparoscopic instruments, and a 26″ LCD monitor. In the case study presented here, the box was a standard training box for laparoscopic surgical training measuring 21.59 cm × cm 31.75 cm × 49.85 cm. Inside the trainer box was a 3D obstacle model composed of rectangular and other shapes. For each individual fixture, a laparoscopic instrument was mounted onto a linear guide that is connected to a gimbal (see Fig. 11). The gimbal and linear guide were connected to optical encoders to measure yaw, pitch, and insertion. The positions in Cartesian space were estimated from the yaw, pitch and insertion measurements by calculating the corresponding Euler angles. The measurement rate was 100 Hz with linear accuracy of ±2 mm. The trainer box was equipped with a Gear-Head WC7351 camera. The 26″ LCD monitor was placed in front of the trainee above the laparoscopic trainer box. It displayed the image generated from the camera as well as three different perspectives of a virtual reality model and shortest paths, which were used as visual guidance for optimal navigation (see Fig. 12).

7.3. Laparoscopic task

The hand–eye coordination task consisted of touching ten target positions in the workspace using the tips of the instruments. The workspace was built with 2 × 2 and 2 × 4 Lego bricks (such elements allow for an quick and easy reconfiguration of the experiment space). The targets for the right and left instruments were marked as L1, L2, . . ., L5 and R1, R2, . . ., R5, respectively. Targets for the right and left hands were simultaneously touched in front of the monitor. Based on visual information, online decisions were made to control the instrument movements.

7.4. Performance assessment

To score performance of each user, metrics, such as total time taken to complete the task and movement economy ratio, were used. Timing score was estimated by subtracting the time to complete the task from a preset cutoff time. To calculate the movement economy ratio, the total optimal path length was divided by the length of paths drawn by the tips of the right and left instruments. The total optimal path length and cutoff time were estimated based on the outputs of the optMIS method. We refer the reader to [17]

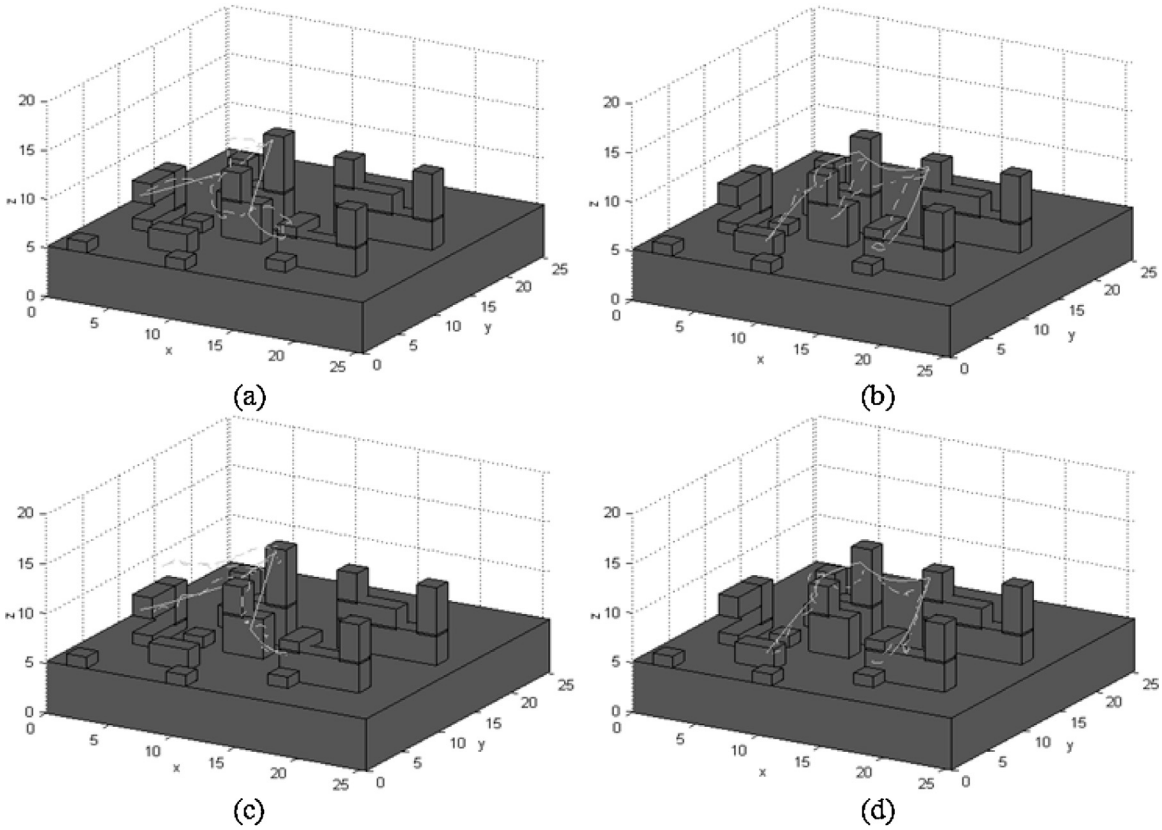

Fig. 13. Shortest (solid line) and actual (dashed line) paths: (a) Scenario 1, left instrument; (b) Scenario 1, right instrument; (c) Scenario 2, left instrument; (d) Scenario 2, right instrument.

for a detailed description of other performance metrics used in the CAST system.

A total score combining the two above scores was calculated for each user. Higher scores correspond to tasks that were completed in a shorter time frame and more accurately.

7.5. Results

In this section, the results achieved in Scenario 1 and 2 are presented. In order to find optimal trajectories that can be used for visual guidance, the 3D obstacle model that replicates the physical model built with Lego bricks was developed. Next, physical constraints of laparoscopic instruments, such as the left and right fixtures, instruments' radius ρ_i, pitching α_i and yawing β_i angles, as well as insertion depths γ_i were defined. Then, the start and goal positions were specified for the left and the right instrument marked as L1 → L2 and R1 → R2, accordingly. Once the input data were provided, the workspace $\mathcal{W}$ was decomposed into a mesh of tetrahedrons *DT*. The lengths of the left $L(F_1)$ and right $L(F_2)$ shortest paths found by the optMIS method were equal to 6.599 cm and 8.887 cm, respectively. The optMIS method was executed four times to find the total shortest paths that connect all target positions. Because of the lack of collisions between the instruments, the time laws were not assigned to the paths.

Once the outputs of the optMIS method were obtained, the hand–eye coordination task was performed using the CAST system. Scenario 1 showed that we faced the problem of analyzing the 3D obstacle space watching the 2D image generated from the camera. The analysis of the motion-tracking data revealed that multiple repetitive movements of the instruments were made to clarify a position in the 3D space (see Fig. 13). The issue with depth perception was causing the discrimination of the distances between backward and forward obstacles. This increased the total time taken to complete the task and resulted in failing to reach the goal positions (i.e., L5 and R5) before the cutoff time. The movement economy ratio varied from 0.41 to 0.52 and from 0.42 to 0.44 for the left and right instruments, respectively, while the desirable value was equal to 1.

Scenario 2 provided a preliminary empirical evaluation of the use of the visual guidance information. We noticed a decrease of total time, while the movement economy ratio lay in the interval 0.43–0.52 and 0.48–0.67 for the left and right instruments, accordingly. Although the total scores of Scenario 2 were higher than the scores of Scenario 1, the performance improvement could be partly caused by the memorization of task settings due to us using the same target positions in both scenarios.

8. Conclusion

In this paper, existing laparoscopy training systems have been analyzed in terms of the representation of the "supervisor". The analysis revealed a high potential for the so called intelligent training systems. Such systems can enable the establishment of proficiency levels for different settings of laparoscopic tasks without involving expert surgeons.

The major contribution of the work is a framework for the transition from surgical training systems in which users are dependent on predefined task settings and lack guidance for optimal navigation of laparoscopic instruments, to the intelligent systems that can potentially deliver the utmost flexibility to the learning process.

A method which provides visual guidance based on optimal navigation was developed by integrating computer simulation and artificial intelligence techniques into a laparoscopic box trainer. In order to guide trainees, the optMIS method was developed to find

the shortest paths in a 3D obstacle space and assign time laws to avoid collisions between laparoscopic instruments. The validation of the method proved its effectiveness in solving optimal motion planning problems. A case study consisting of two task scenarios has been presented. As expected, higher total scores were obtained for the scenario in which visual guidance information was provided. Moreover, the results can be used for further benchmarking of other optimization methods that can be developed for CAST.

We believe that this work will have a broader impact on developing computer-assisted methods for both surgical training and intra-operative support. The optimal trajectories can be used in augmented reality overlays of the training and operative space so that sophisticated visual guidance (akin to that in heads-up displays) is provided. They could also prove useful in pre-operative planning in complex surgical cases to delineate instrument approaches and other steps.

9. Future study

The case study presented in the paper had limitations because trainees memorized particular task settings, which influenced performance results. To avoid this, we plan to perform more experiments for different target positions that are generated randomly in real time. Automatic creation of task settings based on established proficiency levels, is currently under development.

The "time" guidance should be introduced as described in Section 7.1. Visual guidance should be enhanced by including audio signals to notify users that a target position has been reached by the instrument. Finally, haptic feedback should be provided to control the velocity of laparoscopic instruments.

Further progress requires a study involving 30–50 trainees and conducting statistical analysis of the output data.

Acknowledgements

The authors wish to thank Mr. P. Czapiewski of Manufacturing Systems Solutions, LLC for his insightful feedback and mechanical design of our system.

References

[1] N. Stylopoulos, S. Cotin, S.K. Maithel, M. Ottensmeye, P.G. Jackson, R.S. Bardsley, P.F. Neumann, D.W. Rattner, S.L. Dawson, Computer-enhanced laparoscopic training system (CELTS): bridging the gap, Surg. Endosc. 18 (5) (2004) 782–789.
[2] N. Jaber, The basket trainer: a homemade laparoscopic trainer attainable to every resident, J. Minim. Access. Surg. 6 (1) (2010) 3–5.
[3] Y. Al-Abed, D.G. Cooper, A novel home laparoscopic simulator, J. Surg. Educ. 66 (1) (2009) 1–2.
[4] A.M. Derossis, G.M. Fried, M. Abrahamowicz, H.H. Sigman, J.S. Barkun, J.L. Meakins, Development of a model for training and evaluation of laparoscopic skills, Am. J. Surg. 175 (6) (1998) 482–487.
[5] M.S. Wilson, A. Middlebrook, C. Sutton, R. Stone, R.F. McCloy, MIST VR: a virtual reality trainer for laparoscopic surgery assesses performance, Ann. R. Coll. Surg. Engl. 79 (6) (1997) 403–404.
[6] K. Fairhurst, A. Strickland, G. Maddern, The LapSim virtual reality simulator: promising but not yet proven, Surg. Endosc. 25 (2011) 343–355.
[7] LAP Mentor – Simbionix. http://simbionix.com/simulators/lap-mentor (retrieved 11.08.14).
[8] S.A. Fraser, D.R. Klassen, L.S. Feldman, G.A. Ghitulescu, D. Stanbridge, G.M. Fried, Evaluating laparoscopic skills: setting the pass/fail score for the MISTELS system, Surg. Endosc. 17 (6) (2003) 964–967.
[9] World News Laparoscopic Surgery Training. Available from: http://wn.com/laparoscopic_surgery_training
[10] C. Feng, J.W. Rozenblit, A.J. Hamilton, A computerized assessment to compare the impact of standard stereoscopic and high-definition laparoscopic monitor displays on surgical technique, Surg. Endosc. 24 (11) (2010) 2743–2748.
[11] J.R. Korndoffer Jr., J.B. Dunne, R. Sierra, D. Stefanidis, C.L. Touchard, D.J. Scott, Simulator training for laparoscopic suturing using performance goals translates to the operating room, J. Am. Coll. Surg. 20 (1) (2005) 23–29.
[12] L. Beyer, J. De Troyer, J. Mancini, F. Bladou, S.V. Berdah, G. Karsenty, Impact of laparoscopic simulator training on the technical skills of future surgeons in the operating room: a prospective study, Am. J. Surg. 202 (2011) 265–272.
[13] A.M. Spiotta, P.A. Rasmussen, T.J. Masaryk, E.C. Benzel, R. Schlenk, Simulated diagnostic cerebral angiography in neurosurgical training: a pilot program, J. Neurointerv. Surg. (2012).
[14] N.E. Seymour, A.G. Gallagher, S.A. Roman, M.K. O'Brien, V.P. Bansal, D.K. Andersen, R.M. Satava, Virtual reality training improves operating room performance, Ann. Surg. 236 (4) (2002) 458–464.
[15] The Southern Surgeons Club, The learning curve for laparoscopic cholecystectomy, Am. J. Surg. 170 (1995) 55–59.
[16] A.G. Gallagher, J. McGuigan, K. Ritchie, N. McClure, Objective psychomotor skills assessment of experienced, junior, and novice laparoscopists with virtual reality, World J. Surg. 25 (11) (2001) 1478–1483.
[17] M. Riojas, C. Feng, A.J. Hamilton, J.W. Rozenblit, Knowledge elicitation for performance assessment in a computerized surgical training system, Appl. Soft Comput. 11 (4) (2011) 3697–3708.
[18] C.R. Wagner, N. Stylopoulos, R.D. Howe, The role of force feedback in surgery: analysis of blunt dissection, in: Proceedings of the 10th Symposium on Haptic Interfaces for Virtual Environment and Teleoperator Systems (HAPTICS02), 2002, pp. 68–74.
[19] D.H. Lee, J. Choi, J.W. Park, D.J. Bach, S.J. Song, Y.H. Kim, Y. Jo, K. Sun, An implementation of sensor-based force feedback in a compact laparoscopic surgery robot, ASAIO J. 55 (1) (2009) 83–85.
[20] M. Zhou, S. Tse, A. Derevianko, D.B. Jones, S.D. Schwaitzberg, C.G. Cao, Effect of haptic feedback in laparoscopic surgery skill acquisition, Surg. Endosc. 26 (4) (2012) 1128–1134.
[21] P. Strm, L. Hedman, L. Srn, A. Kjellin, T. Wredmark, L. Fellnder-Tsai, Early exposure to haptic feedback enhances performance in surgical simulator training: a prospective randomized crossover study in surgical residents, Surg. Endosc. 20 (9) (2006) 1383–1388.
[22] L. Moody, C. Baber, T.N. Arvanitis, Objective surgical performance evaluation based on haptic feedback, Stud. Health Technol. Inform. 85 (2002) 304–310.
[23] M. Kitagawa, D. Dokko, A.M. Okamura, D.D. Yuh, Effect of sensory substitution on suture manipulation forces for robotic surgical systems, J. Thorac. Cardiovasc. Surg. 129 (2005) 151–158.
[24] S.A. Kobayashi, R. Jamshidi, P. O'Sullivan, B. Palmer, S. Hirose, L. Stewart, E.H. Kim, Bringing the skills laboratory home: an affordable webcam-based personal trainer for developing laparoscopic skills, J. Surg. Educ. 68 (2) (2011) 105–109.
[25] Surgical Science. Available from: http://www.surgical-science.com
[26] R. Aggarwal, P. Crochet, A. Dias, A. Misra, P. Ziprin, A. Darzi, Development of a virtual reality training curriculum for laparoscopic cholecystectomy, Br. J. Surg. Soc. 96 (9) (2009) 1086–1093.
[27] S.M. Lucas, I.S. Zeltser, K. Bensalah, A. Tuncel, A. Jenkins, M.S. Pearle, J.A. Cadeddu, Training on a virtual reality laparoscopic simulator improves performance of an unfamiliar live laparoscopic procedure, J. Urol. 180 (6) (2008) 2588–2591.
[28] G. Sroka, L.S. Feldman, M.C. Vassiliou, P.A. Kaneva, R. Fayez, G.M. Fried, Fundamentals of laparoscopic surgery simulator training to proficiency improves laparoscopic performance in the operating room – a randomized controlled trial, Am. J. Surg. 199 (1) (2010) 115–120.
[29] K.R. Van Sickle, E.M. Ritter, D.A. McClusky, A. Lederman, M. Baghai, A.G. Gallagher, C.D. Smith, Attempted establishment of proficiency levels for laparoscopic performance on a national scale using simulation: the results from the 2004 SAGES Minimally Invasive Surgical Trainer-Virtual Reality learning center study, Surg. Endosc. 21 (2007) 5–10.
[30] D.A. Vincenzi, J.A. Wise, M. Mouloua, P.A. Hancock, Human Factors in Simulation and Training, CRC Press, 2009.
[31] T. Pham, L. Roland, K.A. Benson, R.W. Webster, A.G. Gallagher, R.S. Haluck, Smart tutor: a pilot study of a novel adaptive simulation environment, Stud. Health Technol. Inform. 111 (2005) 289–385.
[32] Simbionix, Procedural Tasks – LapChole, 2005.
[33] Y. Hwang, N. Ahuja, Gross motion planning – a survey, ACM Comput. Surv. 24 (3) (1992) 219–284.
[34] J.P. Desai, Motion Planning and Control of Cooperative Robotic System, University of Pennsylvania, Technical Report No. IRCS-98-27, 1998.
[35] C. Blum, A. Roli, Metaheuristics in combinatorial optimization: overview and conceptual comparison, ACM Comput. Surv. 35 (3) (2003) 268–308.
[36] F. Cazals, J. Giesen, Delaunay Triangulation Based Surface Reconstruction, in: J.D. Boissonnat, M. Teillaud (Eds.), Effective Computational Geometry for Curves and Surfaces, Springer-Verlag, Berlin, Heidelberg, 2006, pp. 231–276, http://link.springer.com/chapter/10.1007%2F978-3-540-33259-6_6
[37] E.W. Dijkstra, A note on two problems in connection with graphs, Numer. Math. 1 (1959) 83–89.
[38] P.S. Hagan, G. West, Interpolation methods for curve construction, Appl. Math. Finance 13 (2) (2006) 89–129.
[39] M. Mitchell, An Introduction to Genetic Algorithms, The MIT Press, USA, 1998.
[40] M. Davoodia, F. Panahib, A. Mohadesc, S.N. Hashemi, Multi-objective path planning in discrete space, Appl. Soft Comput. 13 (1) (2013) 709–720.
[41] F. Cazals, J. Giesen, M. Pauly, A. Zomorodian, The conformal alpha shapes filtration, Visual Comput. 22 (2006) 1–10.
[42] H. Edelsbrunner, E.P. Mücke, Three-dimensional alpha shapes, ACM Trans. Graph. 13 (1994) 43–72.
[43] L. Roditty, U. Zwick, Replacement Paths and k simple shortest paths in unweighted directed graphs, Lecture Notes in Comput. Sci. 3580 (2005) 249–260.